# Chemical/Mechanical Analyses of Anhydride-Cured Thermosetting Epoxys: DGEBA/NMA/BDMA

**Wei Chian† and Delmar C. Timm***

*Department of Chemistry and Chemical Engineering, South Dakota School of Mines, Rapid City, South Dakota 57701, and Department of Chemical Engineering, University of Nebraska−Lincoln, Lincoln, Nebraska 68588*

*Received April 12, 2004; Revised Manuscript Received July 14, 2004*

ABSTRACT: The chemical state of cure in a thermosetting resin was used to predict the resin's equilibrium modulus. High performance liquid chromatography analyses of the sol fraction yielded molar dynamics for monomeric, oligomeric, and polymeric molecules. Their population density distributions were compared with theoretical predictions based on a chain-growth polymerization mechanism. The resulting chemical estimates of the state of cure were integrated into calculations yielding concentrations of network structures within the gel that contribute to the density of elastically active strands and junctions. The theory of rubber elasticity was then used to predict the equilibrium modulus. Measurements incorporated dynamic mechanical analysis. A comprehensive understanding of the polymerization mechanism and cure history are required for accurate simulations of contributions from branch nodes and chain links. Deterministic models based solely on chemical reaction analysis were used to estimate chain connectivity with the gel. Results were interpreted using stochastic-based reasoning.

## Introduction

Research integrated cure dynamics associated with chain structure into predictions of a thermosetting resin's equilibrium modulus.[1,2] The anhydride cured epoxy studied is used as a matrix in high performance, fiber-reinforced composites featuring high specific strength and stiffness and good thermal stability. At elevated temperatures and at high levels of compressive stress at ambient temperature, the molecular structure of the matrix is fundamental to its mechanical properties, which in turn contribute to the performance of the composite.

During the major portion of a cure based on the diglycidyl ether of Bisphenol A (DGEBA), methyl-5-norbornene-2,3-dicarboxylic anhydride, or nadic methyl anhydride (NMA) with the tertiary amine catalyst benzyl dimethylamine (BDMA), Antoon and Koenig[3] observed chemical intermediates that participate in the polymerization reactions. Polyether formation is absent when both monomers are present. Nielsen et al.[4] and Tadros and Timm[5] simplified published reaction schemes to a chain-growth polymerization mechanism where an initiator supplies propagation sites which react with monomers in chain-wise reactions and with oxiranes on molecules in the resin yielding branched and, ultimately, cross-linked chains. Molecules of a similar chemical structure regarding molecular weight and reactive groups were lumped into the dependent variable.

Robbins[6] showed that the expected population density distributions (PDD) are described by the model derived by Fukui and Yamabe.[7] These authors addressed polyether formation using a multifunctional monomer. Robbins et al.[8] demonstrated that deterministically based derivations of post-gel chain topology replicated theoretical results obtained from statistically based methods, including cascade substitution and probability generating functions by Gordon, and co-workers[9,10] and the recursive method introduced by Miller and Makosko.[11,12] Since calculations were based on convergence properties of the moments of the PDD, the procedure is considered to be mathematically intensive. The current work emphasizes branch node dynamics, resulting in models of similar simplicity to that achieved in stochastic based models. Since the theory of rubber elasticity[13−15] incorporates chemical contributions through chain branching and chain segments connecting cross-links, these chemical structures are emphasized in this paper.

Results of a chemical reaction analysis of a thermoplastic resin based on phenyl glycidyl ether (PGE) by Chian and Timm[16] were incorporated into this study. Since the chemical structure of PGE closely resembles that of DGEBA, it is believed that this epoxy monomer serves as a model compound for kinetic reaction studies for the thermosetting DGEBA/NMA/BDMA/IH where the initiator, an alcohol, is IH. PGE contains a single oxirane, whereas DGEBA contains two epoxies. Thus, the former monomer has a functionality of two, and the latter has a functionality of four. Comprehensive analyses of oligomeric distribution dynamics fractionated by reverse phase, high performance liquid chromatography indicated that the rate constant for initiation is distinct from that for propagation. Thus, a Gold[1,17] distribution yields a good estimate of the soluble resin's cure. However, as the average molecular weight of the resin increases with conversion, the two parameter Gold distribution converges to that predicted by the single parameter Poisson distribution.[13,18] Therefore, the latter, simpler reaction mechanism was used in our analyses; i.e., rate constants for initiation and propagation were assumed to be equal. This is also consistent with constraints used in Fukui and Yamabe's[7] derivations.

In our work, three major tasks were addressed. (1) Initially the molar distribution of molecules that com-

* Corresponding author. University of Nebraska−Lincoln.
† South Dakota School of Mines.

10.1021/ma0492925 CCC: $27.50 
Published on Web 09/17/2004

prise the sol fraction was evaluated experimentally and theoretically.[7,19] Objectives included the evaluation of observed/theoretical molecular dynamics in terms of a chain-growth polymerization model. Interpretation of data confirmed the polymerization mechanism, yielded the conversion of oxirane moieties, and provided estimates of the extent of cross-linking. (2) The theory of rubber elasticity[1,2,20] implies that a resin's modulus is fundamentally dependent on covalent bonding through chain connectivity with the gel. Historically, descriptions of contributing chemical structure are based on stochastic and/or hybrid stochastic-deterministic theories. A contribution of this manuscript is an interpretation of gelation theory based solely on chemical reaction analyses coupled to transport phenomena. Derivations are interpreted using statistically based reasoning. (3) The applicability of the theory of rubber elasticity to model the resin's equilibrium modulus was also explored. In this regard, the resin was described in terms of branch node distribution dynamics. The initial task provided for an examination of the reaction mechanism and the extent of cure achieved. In the second and third phases, determinations of cross-link density were integrated into predictions of the equilibrium modulus at temperatures in excess of the resin's glass transition. Determinations based on molecular analyses were compared to macroscopic measurements obtained through dynamic mechanical analysis (DMA).

## Theoretical Considerations

Epoxy/anhydride chemical mechanisms have been discussed by Matějka et al.[21] and Antoon and Koenig.[3] The authors summarized early work in the area. During a major portion of the cure, only carboxylic acid propagation sites are observed, an indication of a rate-limiting step where acid/epoxy reactions slowly form alcohols and alcohol/anhydride reactions rapidly re-form the acid moiety.[4,5] Monomers are coupled through ester bonding. An abbreviated notation was used in describing these reactions. Emphasis is placed on bonding, chemical composition and the chemical functionality of molecules forming the sol. When a carboxylic acid propagation site (I···AH) reacts with an epoxy or oxirane (E), an ester bond and a terminal hydroxyl moiety (I···AEH) form. The latter rapidly reacts with the anhydride (A), forming a second ester and re-forming the carboxylic acid moiety (I···AEAH). The chemical chain structure is $-CH_2CHR_EO\cdots OCR_ACOO-$. The group $R_E$ from DGEBA is pendent to the chain and contains a second epoxy and, therefore, serves as a location for chain branching/cross-linking. With NMA the anhydride residue $R_A$ is integrated into the chain. Thus, the former contributes branch nodes or junctions and the latter contributes chain-links. Because of the rate-limiting reaction assumption, two anhydride links are attached to each reacted epoxy. Their contribution to chain structure was evaluated through stoichiometric considerations. A major experimental/theoretical focus is the reaction extent of the DGEBA branch nodes and their associated chain connectivity within the gel.

DGEBA and NMA are stiff monomers due to cyclic structures, exhibiting a low tendency for intramolecular reactions in their immediate neighborhoods. In derivations of PDD intermolecular reactions are explicit. Intramolecular reactions are implicit, being limited to network formation in the gel. The molar concentration

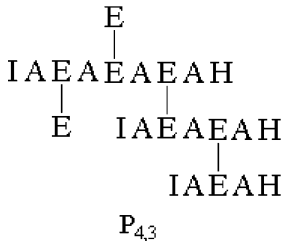


**Figure 1.** Representative molecule $P_{i,j}$ for the resin DGEBA/NMA/BDMA.

of polymeric molecules that contain $i$ DGEBA chain junctions and $j$ propagation sites or branches is expressed as $[P_{i,j}]$. Chemical isomers are lumped into the dependent variable. The monomer DGEBA is labeled $P_{1,0}$; the molecule formed by NMA and an alcohol initiator is $P_{0,1}$. Figure 1 illustrates one configuration for molecules in the collection $P_{4,3}$. Since bonds leading to the gel are absent, molecules are constrained to the sol.

Stoichiometry yields expressions for chemical moieties on molecules in $P_{i,j}$:

oxiranes or epoxies: $$[O_{i,j}] = 2i - (i + j - 1) = i - j + 1$$

esters: $$[\text{ester}_{i,j}] = 2i + 3j - 2$$

phenyls: $$[Ph_{i,j}] = 2i$$

propagation sites: $$[H_{i,j}] = j$$

molar mass: $$MW_{i,j} = MW_A(2j + i - 1) + MW_{E-E}i + MW_{IH}j \quad (1)$$

Initially oxirane groups are considered; originally the $i$ DGEBA units contained $2i$ oxiranes. To connect $i$ units, including $j$ propagation sites, $i - 1 + j$ oxiranes react. Two esters are associated with each reacted oxirane, plus an additional bond forms with each of the $j$ branches. As to phenyl groups, a DGEBA node contains two; NMA is void of phenyls. The number of propagation sites is consistent with the definition of the independent variable $j$. Bonding constraints require $j \geq 1$ and $j - 1 \leq i < \infty$. In a chain-growth cure, any number of monomers may eventually react with a propagation site but a minimum of $j - 1$ nodes are required to connect $j$ propagation sites or branches on a molecule. In modeling, it is convenient to exclude molecules without a propagation site. DGEBA assumes the role of a monomer in typical propagation reactions.

**Population Density Distributions.** The simplified chain-growth reaction scheme, constrained to an alcohol initiator IH, was modeled using these major reactions:

activation: $$IH + A \xrightarrow{\text{fast}} P_{0,1}$$

initiation: $$P_{1,0} + P_{0,1} \xrightarrow{k} P_{1,1}$$

propagation: $$P_{i,j} + P_{1,0} \xrightarrow{k} P_{i+1,j} \quad \text{(monomer)}$$

$$P_{i',j'} + P_{i-i',j-j'} \xrightarrow{k} P_{i,j} \quad \text{(branching)}$$

Constrained by equal reactivity for epoxy groups (i.e., no substitution effect) and equal rate constants for

initiation and propagation reactions $k$, conservation balances[6,7] for a well-mixed, batch reactor yield

$$\frac{d[P_{i,j}]}{k\,dt} = -[H_{i,j}][P_{i,j}]\{\sum_{m=0}^{\infty}\sum_{n=0}^{m+1}[O_{m,n}][P_{m,n}]\} - [O_{i,j}][P_{i,j}]\{\sum_{m=0}^{\infty}\sum_{n=0}^{m+1}[H_{m,n}][P_{m,n}]\} + \sum_{m}\sum_{n}[H_{m,n}][P_{m,n}][O_{i-m,j-n}][P_{i-m,j-n}] \quad (2)$$

The molar concentration of molecules in the collection $P_{i,j}$ is $[P_{i,j}]$; the time is $t$. The three intermolecular rate expressions appearing on the right-hand side of eq 2 represent, respectively, (1) reactions between propagation sites $H_{i,j}$ on molecules $P_{i,j}$ and oxiranes in the resin (sol plus gel), (2) reactions between oxiranes $O_{i,j}$ on the reactant with propagation sites in the resin (a constant), and (3) the formation of molecules $P_{i,j}$ by reactions capable of forming molecules with a degree of polymerization $i$ and $j$ branches. The chemical functionalities of groups participating in the chemical have been defined by eq 1.

Flory[13] argued convincingly that molecules $P_{i,j}$ exist only in the sol. The gel is envisioned as a megamolecule, one that extends at least to the limits of the reactor's dimensions. Subject to this visualization, the initial two rate expressions in eq 2 explicitly address functional groups $H_{i,j}$ and $O_{i,j}$ appearing in the sol on a reactant molecule in $P_{i,j}$. In the accompanying summation expressions, some of their complementary functional groups exist in the sol. These reactions produce a product molecule in the sol at the expense of the two reactants. However, a fraction of the functional groups represented by the summations exist in the gel; thus, a fraction of these reactions transport the reactant from the sol to the gel, adding to the complexity of chain connectivity in the gel and to its mass. However, the solution to eq 2 only requires one to know the total concentration of functional groups in the resin (sol plus gel). The time/conversion transformation required for oxiranes is presented as eq 3, a consequence of any oxirane reacting with any carboxylic acid. Fukui and Yamabe[7] and Robbins et al.[8] developed the solution for $P_{i,j}$ through a proof by induction. Therefore, the population density distribution of molecules within the sol is explicit. However, the molecular chain topology within the gel remains unknown. Conversion does address the competing intermolecular/intramolecular cross-linking reactions. The extent of intramolecular reaction has been recovered through analysis of distinct limits associated with weighted sums of the PDD.[8,13] Developing a description of this chain connectivity is a major emphasis of this paper.

The time/conversion transformation is based on second-order, overall reactions occurring between an invariant number of propagation sites and a time dependent oxirane concentration. Insofar as intramolecular reactions are controlled by collisions resulting from long range, segmental molecular motion and localized group vibrations and rotations, they are expected to be controlled by the same second-order rate expressions that control intermolecular reactions.[13] The constant concentration of propagation sites is expressed as $[P_{0,1}(0)]$; the concentration of oxiranes is expressed through the definition of conversion $\rho$:

$$\rho = (2[P_{1,0}(0)] - \sum_{m=0}^{\infty}\sum_{n=0}^{m+1}[O_{m,n}][P_{m,n}])/2[P_{1,0}(0)] \quad \text{or} \quad \sum_{m=0}^{\infty}\sum_{n=0}^{m+1}[O_{m,n}][P_{m,n}] = 2[P_{1,0}(0)](1-\rho)$$

The oxirane concentration due to intermolecular and intramolecular second-order reactions is expressed through

$$\frac{d\rho}{dt} = k[P_{0,1}(0)](1-\rho) \quad (3)$$

Integration, subject to the initial condition $\rho(0) = 0$, yields

$$\rho = 1 - \exp(-k[P_{0,1}(0)]t) \quad (4)$$

Equation 3 transforms eq 2 from time to conversion space. Sequential integrations yield the population density distribution as a function of conversion. For the initiator $P_{0,1}$,

$$[P_{0,1}] = [P_{0,1}(0)]\exp(-\alpha\rho)$$

The dimensionless quantity

$$\alpha = 2[P_{1,0}(0)]/[P_{0,1}(0)]$$

equals the ratio of epoxy groups to propagation sites which were assumed to equal those introduced in the formulation. The monomer's solution equals

$$[P_{1,0}] = [P_{1,0}(0)](1-\rho)^2 \quad (5)$$

Continuous substitution and solution via integrating factors yield the formula[6,7]

$$p_{i,j} = \frac{[P_{i,j}]}{[P_{1,0}(0)]} = \frac{2j^{i-1}}{(i-j+1)!j!}\alpha^{i-1}\rho^{i+j-1}(1-\rho)^{i-j+1}\exp(-\alpha j\rho) \quad (6)$$

Normalization is based on the initial monomer concentration for DGEBA. A unique feature is the appearance of the exponential term in the PDD when compared with similar expressions descriptive of step-growth polymerizations.[13]

**Critical Conversion.** The conversion when the gel forms has been predicted:[7,8]

$$\rho_c = \left(\frac{[P_{0,1}(0)]}{2[P_{1,0}(0)]}\right)^{1/2} = \frac{1}{\alpha^{1/2}} \quad (7)$$

Although a high initiator concentration is favorable for conversion, see eq 4, it is detrimental to network formation, delaying the gel point $\rho_c$.

**Branch Node Dynamics.** To assist in the development of a description of the extent of cross-linking, the resin is expressed in terms of chain branching dynamics within the sol and the gel. The variable $[N_k]$ represents the concentration of branch nodes. The reaction state of the two oxiranes on DGEBA is bound by $0 \le k \le 2$. The concentration of the monomer $P_{1,0}$ also equals $[N_0]$. Nodes with one and two reacted oxiranes appear in Figure 1 as E−E. Another distinguishing feature of the

cure is that a reacted oxirane contributes a functionality of 2; two chain segments lead away from a reacted moiety.

Subject to the time/conversion transformation eq 3, branch node dynamics were simulated by solving the following equations:

$$\frac{d[N_0]}{dt} = -k2[N_0][P_{0,1}(0)] \quad \text{or} \quad \frac{dn_0}{d\rho} = -\frac{2n_0}{1-\rho}$$

$$\frac{d[N_1]}{dt} = -k[N_1][P_{0,1}(0)] + k2[N_0][P_{0,1}(0)] \quad \text{or}$$

$$\frac{dn_1}{d\rho} = -\frac{n_1}{1-\rho} + \frac{2n_0}{1-\rho}$$

$$\frac{d[N_2]}{dt} = k[N_1][P_{0,1}(0)] \quad \text{or} \quad \frac{dn_2}{d\rho} = \frac{n_1}{1-\rho} \qquad (8)$$

In time space, reactions between epoxies on specified nodes and propagation sites in the resin are modeled in terms of second-order reaction rate expressions; in conversion space, rate expressions simplify to the fraction of oxiranes in the resin appearing on the specified node. The reactions become pseudo-first-order events, $n_0 \rightarrow n_1 \rightarrow n_2$. Normalization is with respect to the initial monomer concentration, $n_k = [N_k]/[P_{1,0}(0)]$.

Expressions in eq 8 yield to interpretations based on transport phenomena. Specifically, the derivative or flux rate for a specified node with respect to reacting epoxies $dn_k/d\rho$ equals the difference between the fraction of oxiranes on a node's precursor when it exists and the fraction of oxiranes on the specified node. In these expressions, the right-hand side represents a gradient with respect to the concentration of moieties on precursors and reactants, analogous to temperature and concentration in energy and mass transport, respectively. The equations' solutions effectively distribute the bonds associated with a specified conversion between the several entities. Subject to an arbitrary but bounded conversion $0 \leq \rho \leq 1$ and initial conditions, $n_0(0) = p_{1,0}(0) = 1$, $n_1(0) = n_2(0) = 0$, solutions equal

$$n_k = \binom{2}{k}\rho^k(1-\rho)^{2-k} \qquad (9)$$

The binomial coefficient equals $2!/(k!(2-k)!)$. When $k = 0$, eq 9 equals eq 5.

**Cross-Link Dynamics.** A node's chain connectivity with the gel contributes to the resin's concentration of elastically active strands and junctions. Published stochastic theories can estimate these quantities. Several authors, including Dotson et al.,[1] state that solutions based on chemical reaction analysis, ie. deterministic-based solutions, are not possible for the calculation of the required chain topology. Earlier, Flory[13] noted that expressions similar to eq 6 for multifunctional monomers only describe molecules within the sol. He argued that gelation theory had to be based on statistics since the gel was excluded. Chain connectivity with the gel was believed to be beyond the realm of chemical reaction theory. Thus, a contribution of our research is the development of a deterministic-based solution. Chemical reaction principles coupled with transport phenomena are explicitly used to distribute bonds between those that lead to chain clusters and those that have attached chain segments leading to the gel. Bonding leading to clusters is referred to as finite and that leading to the gel as infinite.

**Table 1. Structural Denotation of the Cross-Linked Node $X_{k,m}$ [(→) Finite Chain Extensions; (~) Chain Extensions to Gel]**

| $X_{k,m}$ | Extent of Cross-linking, $m$ | | | | |
|---|---|---|---|---|---|
| Reaction State, $k$ | 0 | 1 | 2 | 3 | 4 |
| 0 | E<br>\|<br>E | | | | |
| 1 | ←E→<br>\|<br>E | ~ E→<br>\|<br>E | ~ E~<br>\|<br>E | | |
| 2 | ←E→<br>\|<br>←E→ | ~ E→<br>\|<br>←E→ | ~ E→<br>\|<br>~E→ | ~ E~<br>\|<br>~ E→ | ~ E~<br>\|<br>~E~ |

With advancing conversion nodes $[N_k]$ become partitioned between molecules forming the sol and the gel's network chains. The notation $X_{k,m}$ denotes cross-link nodes or junctions. The subscript $k$ continues to represent the reaction states of the chemical moieties on a node; the subscript $m$ represents the number of attached chains extending from the node to the gel. For the current resin, $0 \leq m \leq 2k \leq 4$. Table 1 provides illustrations of cross-link nodes $X_{k,m}$. The symbol "→" represents an ester bond connected to an anhydride residual that in turn is connected to a finite chain such as those appearing in Figure 1. The notation "~" denotes an ester group leading through an adjoining anhydride link to the gel. Nodes with $m = 1$ are in chain clusters pendent to the network chains. Nodes with two attached, infinite chain segments appear in elastic strands; while nodes with an infinite connectivity exceeding two form elastically active junctions.[1,2,20]

Chain connectivity with the gel is a function of conversion, subject to the polymerization mechanism. Prior to gelation all nodes appear in the sol. After gel formation, intermolecular reactions between chemical groups in the two phases transport all nodes on the soluble molecule to the insoluble gel, forming a pendent chain cluster within the gel. Within this cluster a single path to the gel exists. A subsequent intramolecular reaction involving chemical moieties within this cluster and the gel produces nodes and links with two infinite connections, a strand; however, material will likely remain within the original cluster with but one path to the gel. This may be visualized with the aid of Figure 1 by arbitrarily selecting two chemical moieties to participate in these two events. The chain connecting the two selected sites contains only the nodes with two extensions to the gel. When a third moiety in this cluster experiences an intramolecular reaction, nodes will exist with one, two, and three paths to the gel. On average, chain connectivity is a function of the distribution of bonds existing at the time of their formation. The distribution of nodes within the resin is described by eq 9.

In developing a deterministic theory that describes the distribution of ester groups leading to finite and infinite structures, conversion is initially specified, which in turn freezes chain connectivity. If the selected conversion is less than the critical conversion (eq 7), all bonds appearing on nodes $[N_k]$ are assigned to cross-links $X_{k,0}$. The complement addresses that condition after gelation. During the cure the distribution of the nodes with $k$ reacted sites and $m$ ester bonds leading to the gel were formed through an initial intermolecular sol/gel reaction. Subsequent intramolecular reactions continued dynamics associated with chain connectivity.

**Table 2. Concentration Distribution of Cross-Linking Nodes $X_{k,m}$**

| | distribution of $X_{k,m}$ | | | | |
|---|---|---|---|---|---|
| reaction state, $k$ | $m = 0$ | $m = 1$ | $m = 2$ | $m = 3$ | $m = 4$ |
| 0 | $(1-\rho)^2$ | | | | |
| 1 | $2\rho(1-\rho)(1-\rho_x)^2$ | $4\rho(1-\rho)\rho_x(1-\rho_x)$ | $2\rho(1-\rho)\rho_x^2$ | | |
| 2 | $\rho^2(1-\rho_x)^4$ | $4\rho^2\rho_x(1-\rho_x)^3$ | $6\rho^2\rho_x^2(1-\rho_x)^2$ | $4\rho^2\rho_x^3(1-\rho_x)$ | $\rho^2\rho_x^4$ |
| | sol | | gel | | |

[a] $m$ = extent of cross-linking.

Reactions at the node and at neighboring nodes contribute to the network chain topology through covalent bonding and associated chain connectivity, but the ultimate dependency solely rests on the extent of reaction for a given chemical reaction mechanism. Analogies addressing cross-linking with conversion, as expressed in eq 8, are now developed.

In eq 8, time is initially explicit. After the transformation to conversion space, one arbitrarily selects a conversion, subject to initial conditions defining the number of groups capable of reacting with the invariant propagation sites and the initial distribution of moieties among the several nodes $N_k(0)$. For a formulation where only monomers exist, $[N_k(0)] = 0$ except for $[N_0(0)] > 0$. When a distribution of polymer molecules exist with the monomer, initial conditions will reflect their extent of branching at time zero. The transformed, ordinary differential equations in conversion space distribute bonds corresponding to the conversion $\rho$ selected from among the epoxy moieties that initially existed; see eq 8. Although time is of no consequence, one may recover the time required to achieve the conversion of the oxiranes; see eq 4. The significant observation is that this chemical reaction allocation of bonds obeys a series of first-order events, $n_0 \rightarrow n_1 \rightarrow n_2$.

In cross-linking space analogous allocations of existing bonds are envisioned. One needs to distribute finite bonds to infinite bonds on a specified node. Specific details associated with reactions are not explicitly required. One needs to know only the extent of reaction. An arbitrary conversion greater than the critical conversion is specified and held constant. A series of first-order transformations are envisioned that distribute existing esters between attached finite and infinite structures; $X_{k,0} \rightarrow X_{k,1} \ldots \rightarrow X_{k,2k}$. The invariant value for k is consistent with the frozen extent of reaction of oxiranes. This series of first-order events leads to a set of equations analogous to eq 8:

$$\frac{\partial x_{k,m}}{\partial \rho_x} = -\frac{2k-m}{1-\rho_x}x_{k,m} + \frac{2k+1-m}{1-\rho_x}x_{k,m-1}(1-\delta_{0,m}) \tag{10}$$

$$x_{k,m}(0) = n_k\delta_{0,m} \quad \text{and} \quad 0 \le m \le 2k \le 4$$

In eq 10, $x_{k,m}$ is the normalized concentration of the nodes $[X_{k,m}]/[P_{1,0}(O)]$. The variable $\rho_x$ is the extent of cross-linking, the fraction of bonds that lead to the gel at conversion $\rho$. The fraction of bonds leading to finite chain clusters is $(1 - \rho_x)$. Since existing bonds are addressed in cross-linking space, the partial derivative indicates constant $\rho$ and $k$. The extent of cross-linking is a function of conversion. This will be addressed.

Rate expressions on the right side of eq 10 equal the fraction of finite bonds on the specified node. Thus, the rate of change in the concentration of nodes having $k$ reacted oxiranes and $m$ infinite extensions due to the extent of cross-linking $\partial x_{k,m}/\partial \rho_x$, is positively influenced by the rate of transport addressed by the fraction of finite bonds in the resin on precursors $x_{k,m-1}$ and is negatively influenced by the fraction of finite bonds on the specified node $x_{k,m}$. The Kronecker $\delta$ function equals

$$\delta_{k,m} = \begin{cases} 1 & k = m \\ 0 & k \neq m \end{cases}$$

The Kronecker containing function equals zero when precursors do not exist at permissible $k$'s but $m = 0$. Null initial conditions exist except when $m = 0$ where $x_{k,0}(0) = n_k$, the concentration of nodes at $\rho$ that exist with $k$ reacted epoxies, see eq 9. These functions of conversion $n_k$ are constants in extent of cross-linking space since conversion is invariant. The inequalities in eq 10 emphasize that nodes in the sol have finite chain extensions and that nodes in the gel have varying extents of connectivity with the gel that depend on the extent of reaction $k$ of the node and conversion.

Solutions to eq 10 are now illustrated. When $k = 0$, the DGEBA monomer is addressed; in the absence of bonds, the right-hand side of eq 10 equals zero. Integration yields $x_{0,0} = n_0 = n_0(0)(1 - \rho)^2$, a constant in extent of cross-linking space. The solution is provided by eq 9. When $k = 1$, up to two infinite chain extensions can exist. Initially eq 10 is solved for $m = 0$:

$$\partial x_{1,0}/\partial \rho_x = -2x_{1,0}/(1-\rho_x); \quad x_{1,0}(0) = n_1$$

Integration coupled with algebra yields $x_{1,0} = n_1(1 - \rho_x)^2 = n_0(0)2\rho(1 - \rho)(1 - \rho_x)^2$. Next eq 10 is constrained by $k = m = 1$:

$$\partial x_{1,1}/\partial \rho_x = -x_{1,1}/(1-\rho_x) + 2x_{1,0}/(1-\rho_x); \quad x_{1,1}(0) = 0$$

Subject to the zero initial condition, integration using an integrating factor yields $x_{1,1} = n_1 2\rho_x(1 - \rho_x)$. Solutions to eq 10 equal

$$x_{k,m} = n_k\binom{2k}{m}(1-\rho_x)^{2k-m}{\rho_x}^m \quad \text{subject to } 0 \le m \le 2k \le 4 \tag{11}$$

Solutions appear in Table 2, the theoretical concentration distribution of cross-linked nodes at conversion $\rho$.

In the interpretation of experimental data, the sol fraction was used to evaluate the extent of cross-linking $\rho_x$ at conversion $\rho$. The column labeled sol in Table 2 defines the portion of the sol $w_s$ associated with branch nodes including the monomer. Addition, subject to factoring, yields

$$w_s = [(1-\rho) + \rho(1-\rho_x)^2]^2 \tag{12}$$

A stochastic interpretation of this solution follows. Initially the reaction state of an oxirane contributed by DGEBA is considered. The probability that an epoxy

group is not reacted equals the fraction $1 - \rho$. Since oxiranes do not contribute infinite chain extensions, the likelihood that it is connected to finite chain clusters is 100%, resulting in a coefficient of 1 for this term in eq 12. The complement, the likelihood that the selected epoxy has reacted, is $\rho$. A reacted oxirane is connected to two ester bonds. The fraction $1 - \rho_x$ equals the probability that one ester leads into a chain cluster. The cross-linking states of both bonds are independent events, resulting in the expression in eq 12 being squared. For the node to be in the sol, both oxirane groups on DGEBA have to contribute finite structures. Each contributes an independent event, resulting in the final power of 2 in eq 12.

**The Prediction of the Modulus.** The terms in the columns labeled gel in Table 2 are used to calculate the several dependent variables needed in the prediction of the rubbery equilibrium modulus. Dotson et al.[1] and Mark and Erman[18] summarized molecular contributions to the equilibrium tensile modulus $E$ through the expression

$$E = 3(\upsilon_c - h\mu_c)RT + T_e E^\circ \qquad (13)$$

Chemical contributions associated with bonding are contained in the initial term. The variable $\upsilon_c$ represents the concentration from elastically active strands while $\mu_c$ defines contributions from elastically active junctions. The junction fluctuation parameter $h = 0$ when the model is affine; when $h = 1$, the model is phantom. The final expression represents the contributions from permanent, physical chain entanglements. The entanglement trapping parameter is $T_e$, and the plateau modulus of an un-cross-linked, high molecular material formed from the network strands is $E^\circ$. The ideal gas constant is $R$, and the absolute temperature is $T$.

An elastically active junction contains three or more paths to the gel. Therefore, their normalized concentration equals

$$\mu_c = x_{2,3} + 2x_{2,4} = 2\rho^2\rho_x{}^3(2 - \rho_x) \qquad (14)$$

A junction with four attached strands is considered to be twice as effective as a junction with three attached strands. Strands connect two elastically active junctions:

$$\upsilon_c = (3x_{2,3} + 4x_{2,4})/2 = 2\rho^2\rho_x{}^3(3-2\rho_x) \qquad (15)$$

Weights equal the number of strands attached to the node; the denominator is a consequence of a strand connecting two active nodes. Cross-links with fewer attached strands are either in a strand or in a pendent chain cluster.

Chain entanglements are arbitrarily assumed to occur between two anhydride links. In order for an entanglement to be permanent and to contribute to the equilibrium modulus, all four exiting chain segments on the two entangled molecules must extend to the gel. With the aid of entries in Table 2 and solutions provided by eq 11, one may initially ask the question: What does the fraction of bonds leading from the gel into nodes with exiting finite attachments equal? The solution $4\rho\rho_x(1 - \rho_x)(1 - \rho + \rho(1 - \rho_x)^2)$contains contributions from $X_{1,1}$ and $X_{2,1}$. The weight $4\rho\rho_x = \sum_{k=1}^{2}\sum_{m=1}^{2k} m\ x_{k,m}$ equals the fraction of bonds leading to the gel. In reference to Table 1 and Figure 1, esters are being counted twice per reacted oxirane. Normalization with respect to $4\rho\rho_x$ produces the probability of randomly selecting an ester that comes from the gel and enters a node with finite attachments. The likelihood of selecting an ester connected to the gel that leads through the node to the gel is one minus this normalized quantity, yielding

$$T_e = [1 - (1 - \rho_x)(1 - \rho + \rho(1 - \rho_x)^2)]^4 \qquad (16)$$

The two entangled anhydrides offer four chain segments associated with their two chains. Since each direction provides an independent event, the difference in eq 16 is raised to the power of four. The expression $1 - \rho_x$ is the probability that the chain segment entering from the entanglement through the reacted oxirane has a finite continuation. The quantity within the second parenthesis represents the reaction state of the second oxirane on the node. If it is an oxirane, the path to it leads to a finite entity and thus $1 - \rho$. If this moiety has reacted, both attached esters must lead to chain clusters. These are three independent events and, therefore, they are multiplied. Dotson et al.[1] and Miller and Macosko[12] report similar expressions, subject to different polymerization mechanisms, derived from stochastic based arguments used in our interpretation.

## Experimental Section

**Preparation of Resins.** The purity of the raw materials and suppliers were (1) DGEBA (Der Resin 332, 346−350 Da, Sigma Chemical Co.), (2) methyl-5-norbornene-2,3-dicarboxylic anhydride or NMA (89.5%/titration or 93.4%/chromatography, 178.19 Da) and (3) BDMA (99.0% min, 0.2% max moisture, 135.21 Da) (certified ACS, Aldrich Chemical Co.). A chromatogram was observed for DGEBA. One major peak and a minor peak were observed. Following Shiono et al.[22] and Dark et al.[23] the minor component is believed to be 2,4-bis(α,α-dimethyl-*p*-hydroxylbenzyl)phenol. The anhydride and catalyst produced single GPC peaks. For a near stoichiometric epoxy/anhydride ratio, 26.78133 g of DGEBA was weighed in a tared beaker. Next 27.45776 g of NMA was added, followed by 1.02599 g of BDMA, resulting in a molar ratio of 0.4995/1.0/0.049 for illustration. A unique feature for this anionic, chain-growth resin formulation is that excess anhydride simply remains at 100% conversion of oxiranes. If the anhydride is limiting, the reaction ideally stops at 100% conversion. In reality, polyethers may form.[3] The consequences are minor compared to those associated with an imbalanced stoichiometry for step-growth polymerization mechanisms. Care was exercised to achieve a balanced stoichiometry. Because of the presence of impurities, the formulation will cure without the addition of an initiator. An alcohol, 2-ethylhexanol, acted as an initiator and was added to the extent that its molar ratio varied from 0.005 to 0.05 to prepare resins of relatively high or low molecular weight, respectively. After mixing, a master batch was subdivided into 5 mL vials and placed in a preheated electric oven with air circulation set at 80 °C. Curing reaction mixtures were collected at preset time intervals, thermally quenched and stored at −10 °C.

**GPC—MALLS.** The GPC system consisted of three Waters 7.8 × 300 mm columns (Styragel, HR 0.5, HR1.0 and HR 2.0), a Waters chromatograph pump (model 590), a miniDAWN laser light scattering photometer (Wyatt Technology), and a Waters 410 differential refractometer. HPLC grade toluene (Aldrich Chemical Co.) was used as the mobile phase at a flow rate of 0.75 mL/min. A Millipore in-line 0.2 μm filter was placed between the pump and the injector. The detectors were computer interfaced with ASTRA software which controlled the acquisition of data and processed the data to obtain molar masses and other results. GPC-MALLS samples for soluble resins were prepared by dissolving 0.1 g of reaction mixture in 5 mL of toluene (HPLC grade, Aldrich Chemical Co.) and

injected in the amount 100 $\mu$L. DGEBA/NMA/BDMA reaction mixtures collected after gelation were first leached with toluene (1−10 g resin in 20 mL of solvent depending on the depth of cure) and injected in the amount 100 $\mu$L.

**DMA.** The dynamic mechanical analysis (DMA) used a TA Q 800 instrument. Specimen dimensions were 17.5 × 12 × 3.5 mm. A single cantilever clamp was used. Scans at 3 °C/min were from ambient temperature to approximately 200 °C using a 15 $\mu$m amplitude at 1 Hz. An inert nitrogen atmosphere was used. Specimens were machined from flat sheets; edges were smoothed with sandpaper.

## Results and Discussion

**Oxirane Dynamics.** Polymerizations were observed as a function of time for two reaction mixtures. Resin samples collected near or beyond the gel point were first weighed, $W_{samp}$, and then leached with HPLC grade toluene in a stainless steel bomb at temperatures near their glass transition temperatures for 2 h. The sol was filtered from the gel. The gel was washed four times to remove soluble material and then vacuum-dried for 24 h and weighed $W_{d,g}$. The weight fraction of the sol fraction $w_s$ equals

$$w_s = 1 - W_{d,g}/W_{samp}$$

On the basis of the initial composition of the reaction mixture, the mass of the resin is

$$W_{resin} = [P_{1,0}(0)](MW_{E-E} + 2MW_A) \qquad (17)$$

Equations 17 and 18 were used to calculate the initial moles of DGEBA, $[P_{1,0}(0)] = [N_o(0)]$.

The monomer's weight fraction in the sol was evaluated through GPC fractionations:

$$w_{E-E} = \frac{\text{area}_{DGEBA}/\alpha_{E-E}}{(\text{area}_{DGEBA}/\alpha_{E-E}) + (\text{area}_{NMA}/\alpha_A) + (\text{area}_{oligomers}/\alpha_{oligomers})} \qquad (18)$$

The extinction coefficients for NMA, DGEBA, and oligomers are $\alpha_A$, $\alpha_{E-E}$ and $\alpha_{oligomers}$. They were determined by performing GPC analyses on a series of solutions with known concentrations. The analysis for the oligomers used the same reaction mixture. The molar concentration for DGEBA equals

$$[P_{1,0}] = \frac{w_{E-E} w_s W_{samp}}{MW_{E-E}} \qquad (19)$$

The conversion of epoxide groups $\rho$ was calculated using eq 5:

$$1 - \rho = \left(\frac{[P_{1,0}]}{[P_{1,0}(0)]}\right)^{1/2} \qquad (20)$$

In Figure 2, two oxirane decay curves may be observed to be consistent with eq 4 for appreciable reaction times for resins with two different IH/epoxy concentrations, 0.01 and 0.10 (or $\alpha = 200$ and 20). The slopes are in the ratio of approximately 6/1, whereas the formulated initiator ratio was 10/1. The monomers are known to contain impurities that act as initiators. If considered, these contaminants including 2,4-bis(α,α-dimethyl-*p*-hydroxylbenzyl)phenol and moisture in BDMA will cause a reduction in the 10/1 ratio.

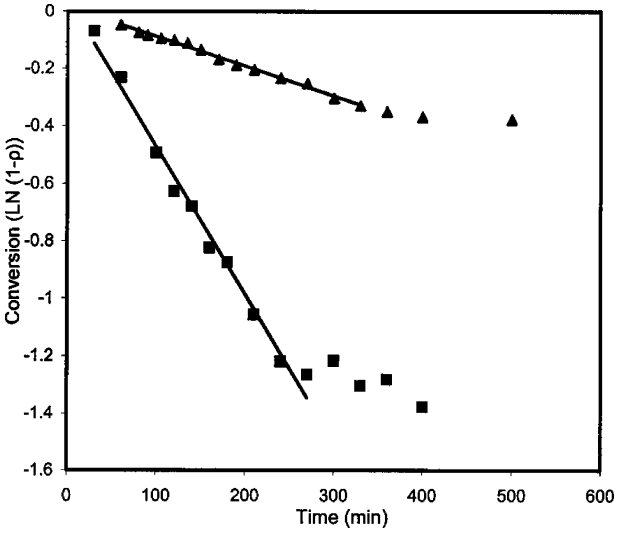


**Figure 2.** Decay dynamics of epoxy groups at 80 °C (▲, $\alpha$ = 200; ■, $\alpha$ = 20).

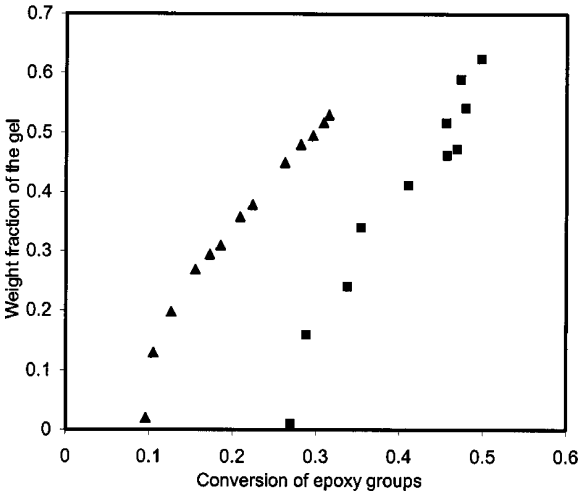


**Figure 3.** Evolution of the sol/gel partition of DGEBA/NMA/BDMA (▲, $\alpha$ = 200; ■, $\alpha$ = 20).

The rate of decay of epoxy groups decreased appreciably at higher conversions due to the overall reaction becoming diffusion-controlled[24−26] at the reaction temperature. The curing resin's glass transition temperature approached 80 °C. Initiator concentration had a pronounced effect on cure and cross-link structure as evident from the distinct conversions.

The relative ratio of initiator/monomer strongly influenced the rates for propagation and intermolecular additions. In the polymerization with 0.01 initiator, propagation is preferred on a stoichiometric basis and resulted in gelation from a few macromolecules at $\rho_c$ = 0.07. The resin with the higher initiator/monomer concentration of 0.10 resulted initially in more oligomeric molecules due to the faster rate of conversion, but gelation was delayed to $\rho_c$ = 0.22. Similar trends are associated with vitrification. The increase in initiator concentration favors branching. The resulting chain topology had a significant influence on gelation and the development of a glass transition temperature with respect to conversion.

**Sol/Gel Partition.** Gel points $\rho_c$ were determined by extrapolating observed gel fractions $w_g = 1 - w_s$ to zero; see Figure 3. Experimental gel points are tabulated in Table 3 as are theoretical predictions of critical conver-

**Table 3. Gel Point Conversion of Epoxide Groups for $E_2$ + A**

| | critical conversion $\rho_c$ | |
|---|---|---|
| ratio $\alpha^a$ | exptl | theor |
| 200 | 0.096 | 0.0707 |
| 20 | 0.254 | 0.2236 |

[a] Ratio $\alpha = 2[P_{1,0}(0)]/[P_{0,1}(0)]$.

sions based on eq 7. Measured gel points were higher than predicted values when formulated initiator concentrations were used in calculations. Impurities present in monomers lead to lower actual values for α. Therefore, predictions of the gel point are known to be too low. Nonetheless, experimental−theoretical comparison suggests that the greatly simplified overall kinetic reaction model satisfactorily approximates the gel point for this resin. Gel points are used as a quality control indicator in manufacturing. Equation 4 can be used to predict pot life.

A second factor to be considered when estimating gel points is the influence of chain cyclization in the sol. The constraint of no intramolecular reactions during derivations of PDD may not be absolutely valid. Chain cyclization delays gelation inasmuch as this intramolecular reaction reduces elastically active junctions.[1,27] However, ring structures present in the monomers appreciably stiffen chains; and, therefore, local chain cyclization is not expected to be significant. A third consideration lies in the constraint of rate constants independent of chain length. The assumption appears to be valid for the DGEBA/NMA/BDMA resin, at least in the neighborhood of the critical conversion. If the apparent reactivity of groups on larger molecules were significantly lower compared to the reactivity of groups on smaller molecules, the gel point conversion would be shifted to higher values.[28] Conversion would not be exponential in time. A contributing factor could be associated with steric hindrance, or molecular diffusion as with the Trommsdorff effect in chain-growth reactions. However, the gel points are near 50 (α = 20) and 140 min (α = 200) in Figure 2. They are far removed from the conversions where the overall reaction becomes diffusion-controlled (near 250 and 400 min in Figure 2). Monomer dynamics in time are not impeded at the critical conversions.

**PDD Analysis.** DGEBA/NMA/BDMA/IH resins of various degrees of cure were analyzed by GPC−MALLS, obtaining cumulative weight vs molecular weight distributions. Before reaching the critical conversion, the cured resin was totally soluble and measured molar mass distributions were representative of the resin. At higher cures, experiments determined the molecular weight distribution of the sol. A series of cumulative molar mass distribution curves with an initial IH/DGEBA ratio of 0.01 is presented in Figure 4. A soluble series of samples cured for 60, 80, 100, 120, and 135 min of progress from left to right with approximate average molecular weights of 7000, 8500, 9500, 12000 and 14000. The narrow distribution (polydispersity less than 1.1) is readily apparent in the sample cured for 135 min, the curve on the far right.

After gelation, the molecular weight distribution of the sol shifted back toward lower molecular weights with increasing degree of cure (9500, 2500, and 1600 Da at 150, 190, 300 min, respectively). Because of a larger number of chemical functionalities (eq 1), higher molecular weight polymeric molecules experience a proportionately greater rate of transport to the gel. Molecules of the order of 10 000 Da were present. The theoretical population density distribution eq 6 predicts a higher concentration of polymeric molecules than is experimentally observed. Results are shown in Figure 5. Simulations presented explored the effect of the initial oxirane/initiator ratio. The lower molecular weight molecules are reasonably approximated by eq 6, weighted by eq 1, when α = 160 to 175 and $\rho_c$ is close to 0.08 (instead of 0.07 when α = 200), a value near the experimental $\rho_c = 0.10$.

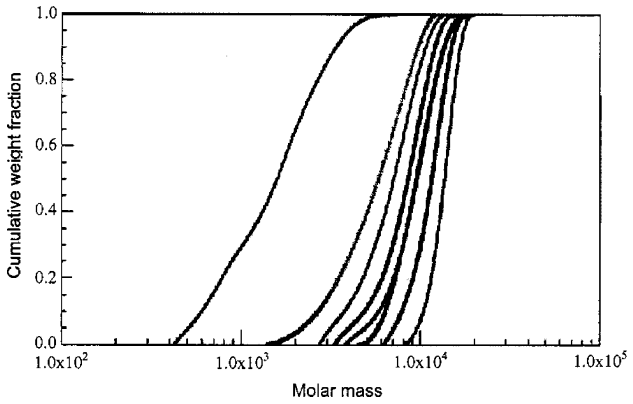


**Figure 4.** Evolution of molecular weight distribution of DGEBA/NMA/BDMA Reaction (IH/DGEBA ratio 0.01 at 80 °C. Right to left: 135 min, 120 min, 100 min, 150 min sol, 80 min, 60 min, 190 min sol, 300 min sol).

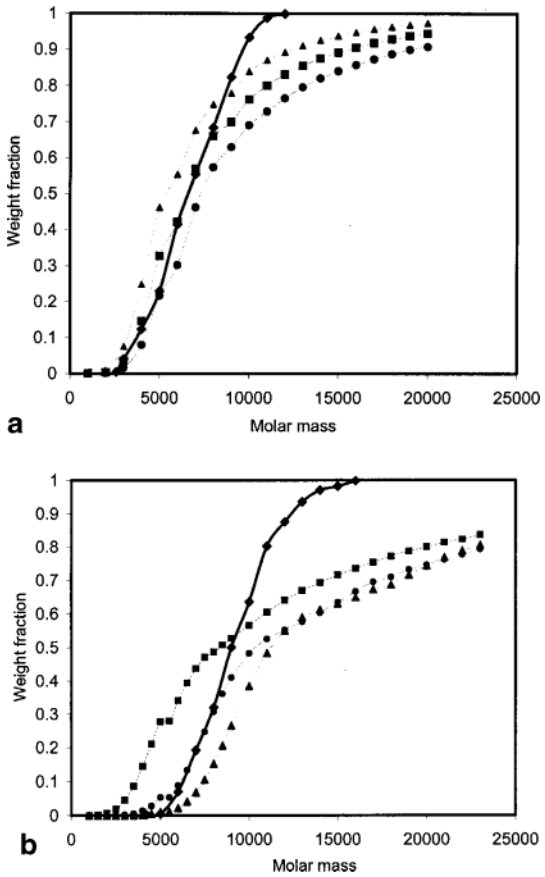


**Figure 5.** Molecular weight distribution of DGEBA/NMA/BDMA: (a) initiator/DGEBA ratio 0.01, 60 min at 80 °C [(◆) experimental; theoretical (●) α = 200, (■) α = 150, (■) α = 175]; (b) initiator/DGEBA ratio 0.01, 100 min at 80 °C [(◆) experimental; theoretical (●) α = 160, (▲) α = 200, (■) α = 120).

The GPC−MALLS interpretation of chromatograms relied on eq 6 for oligomeric fractions, subject to eq 1 for average molecular weights of molecules $P_{i,j}$. Experimental/theoretical molecular weight distributions offer insight into reaction kinetics and mechanisms. The weight fraction of molecules $P_{i,j}$ was calculated by

$$\frac{W_{i,j}}{W_{resin}} = \frac{MW_{i,j}p_{i,j}}{\sum_{i=1}^{\infty}\sum_{j=1}^{\infty} MW_{i,j}\cdot p_{i,j}} \tag{21}$$

where $W_{i,j}$ denotes the mass of molecules $P_{i,j}$ in the sol. The variable α appearing in eqs 6 and 7 was initially set by the chemical composition of the formulated mixture (assuming impurities are absent). Conversion $\rho$ was determined using eq 20 based on the GPC fractionation of DGEBA. Resultant weights were sorted solely as a function of molecules' molecular weight, yielding the cumulative mass distribution curves of Figure 5, parts a and b, comparisons between theoretical and experimental curves for two representative cures before gelation. Three fitting curves are presented in each figure. The original curve based on the initial ratio of epoxide groups to propagation sites (α = 200) departs substantially from the experimental curve. Some improvement is realized when the initiator is increased by using a lower value for the parameter α. For example, in Figure 5b, the fitting curve with α equal to 120 has an average molecular weight that is close to the experimental curve. On the other hand, the theoretical curve with α equal to 160 fits the experimental curve for a major part of the low to middle molecular weight range. Similar observations apply to Figure 5a, a sample collected at a lower conversion. A mean value for α = 160 is reasonable based on the fitting of oligomers. This analysis also illustrates the use of molecular data in a feed-back sense in critical assessments of the cure and formulation. Such can be incorporated into quality control before and after gelation. Thermosets are not precisely intractable resins.

**Examination of Constraints.** The kinetic model predicts molecular weight distributions broader than the experimental distributions. Similar trends were reported for the thermoplastic analogue based on phenyl glycidyl ether, PGE/NMA/BDMA/IH.[16] A minor, competing reaction that diminishes the number of molecules and narrows the PDD seems to be present. When examining oligomeric dynamics, the two parameter Gold[17] distribution was appropriate for the thermoplastic resin. The rate constant for initiation was approximately 3−4 times greater than the rate constant for propagation. A slower propagation rate compared to initiation rate leads to molecular size distributions narrower than the Poisson distribution at lower reaction extents.[16] However, at reasonable conversions, the Gold distribution converges to the single parameter Poisson distribution.[1,18] The constraint of a single rate constant was applied in developing eq 6.[6,7] For the thermosetting resin, the effect on PDD of this constraint has not been simulated.

The kinetic model includes both chain extension reactions between the monomer and propagation sites and polyaddition reactions that yield branched and cross-linked chain configurations. The PGE examination implies that the rate constants are equal after the initial addition of a chain link. DGEBA has been reported to be void of first-shell substitution effects;[29,30] thus, monomeric and pendent oxiranes are believed to have the same chemical reactivity. Therefore, the two reactions were assumed to proceed with identical rate constants. Chromatograms in Figure 6 correspond to resins at IH/DGEBA = 0.01 collected at 105 and 360 min, respectively. The former sample precedes gelation; the latter is after the formation of gel. The ratio of anhydride to epoxy changed in this time interval. DGEBA was consumed faster than NMA. An interpretation was based on eq 5, subject to constraints that

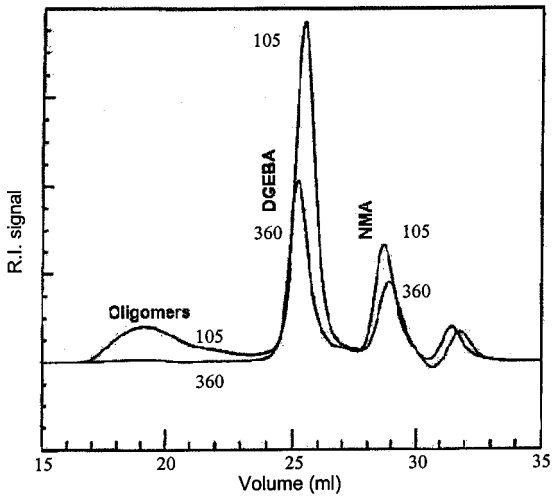


**Figure 6.** GPC chromatograms of DGEBA/NMA/BDMA reaction mixtures (initiator/DGEBA ratio 0.01, 80 °C).

$$\frac{(1-\rho)_1}{(1-\rho)_2} = \frac{\text{area}_{\text{DGEBA},1}}{\text{area}_{\text{DGEBA},2}} = \frac{\text{area}_{\text{NMA},1}}{\text{area}_{\text{NMA},2}}$$

On average, the left side equals 1.8 and the right side is near 1.4. This may imply that reaction rate constants are slightly different. Conceivably, the reactivity of the DGEBA monomer with propagation sites may be higher than that for the polymeric/polymeric coupling due to the monomer's smaller size and hence increased mobility. The formation of relatively compact, highly branched molecules may be less favored than is the formation of relatively long chains with pendent oxiranes. A reduction in the rate of reaction for pendent oxiranes will result in an accumulation of NMA relative to DGEBA in the absence of either formation.[3,19] Figure 1 may be consulted.

Inspection of Figure 6 also reveals the rapidly diminishing oligomeric fraction within the sol. Relatively large quantities of resin must be leached to achieve sufficient quantities for analyses. Research in progress is drying the sol fraction so that its concentration can be manipulated to better fulfill concentration requirements for the GPC−MALLS analyses.

**The Extent of Cross-Linking.** At the gel point, the viscosity of the material diverges, and a modulus begins to appear. Elastically active strands, elastically active junctions, and chain entanglements contribute to the equilibrium tensile modulus $E$; see eq 13. These variables have been correlated to sol/gel partition properties by the branching theories discussed. Results expressed by eqs 8 and 11 are summarized in Table 2.

The extent of cross-linking $\rho_x$, the fraction of bonds that lead to the gel, was interpreted from the experimental measurement of the soluble weight fraction $w_s$

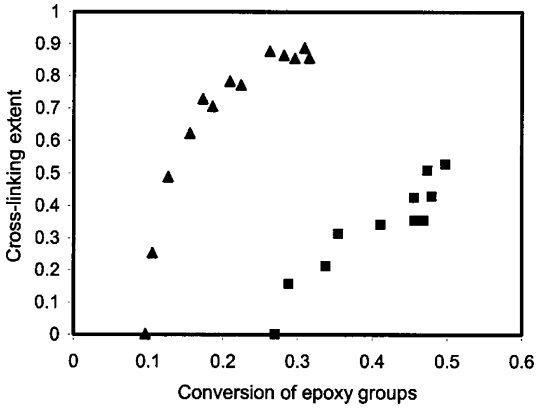


**Figure 7.** Cross-linking dynamics at 80 °C (▲, α = 200; ■, α = 20).

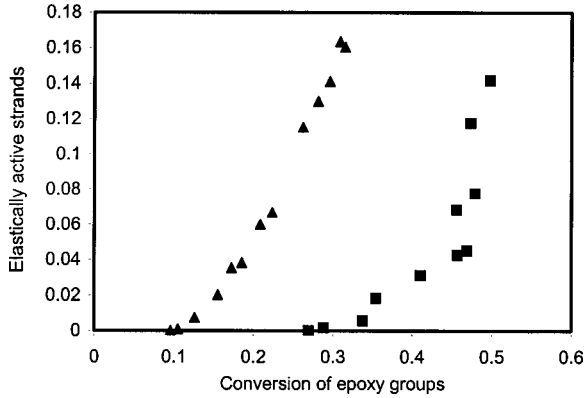


**Figure 8.** Theoretical growth of elastically active strands (▲, α = 200; ■, α = 20).

and the conversion of epoxide groups. Equation 12 is on a DGEBA basis. Stoichiometry, see Figure 1 and eq 1, was used to determine the anhydride content of the sol. Figure 7 presents results for the extent of cross-linking as a function of conversion of epoxy groups. A higher cross-link density was achieved with the low initiator concentration at low conversions. In higher molecular weight strands, proportionately more bonds lead to the gel. This is consistent with prior discussions addressing chain configurations. Also, initiator residues become dangling ends, disrupting network development even at 100% conversion in this resin system.

**The Rubbery Equilibrium Modulus.** On the basis of measurements for conversion $\rho$ and the extent of cross-linking $\rho_x$, the terms appearing in Table 2 were calculated, yielding quality estimates for the distribution of cross-link nodes $X_{k,m}$. Figure 8 presents the theoretical growth of elastically active strands $\upsilon_c$, subject to eq 15, with varying initiator content. The evolution of elastically active junctions, $\mu_c$, was calculated from eq 14 and is plotted in Figure 9. Predictions of chain entanglement trapping factors $T_e$ utilized eq 16 and are shown in Figure 10. The diminished gel structure at a given conversion caused by an increased initiator concentration is readily apparent in the three graphs. The likelihood of entering a chain cluster is substantial. During processing, such as filament winding, care must be exercised to limit impurities such as moisture from the roving. Moisture is a potential initiator; the resin is hydrophilic. Moisture will cause a reduction in the shear modulus.

DMA experiments measured three equilibrium rubber moduli of nonextracted DGEBA/NMA/BDMA/IH resins,

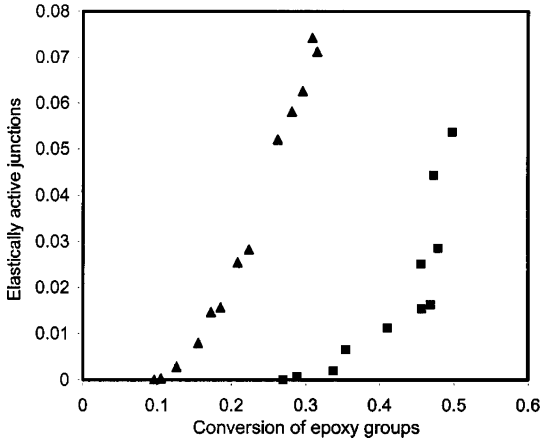


**Figure 9.** Theoretical growth of elastically active junctions (▲, α = 200; ■, α = 20).

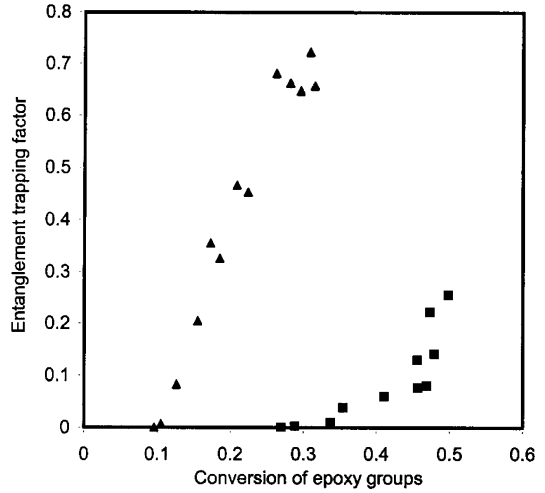


**Figure 10.** Prediction of entanglement trapping factor (▲, α = 200; ■, α = 20).

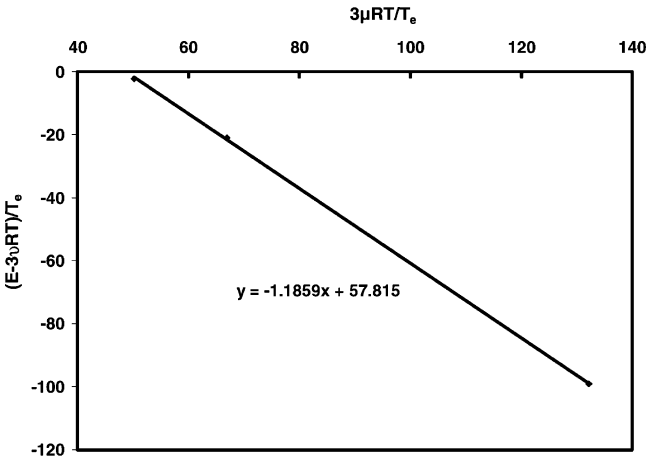


**Figure 11.** Experimental−theoretical comparison of rubber equilibrium modulus (assuming an affine network).

α = 200. For the experimental−theoretical comparison shown in Figure 11, eq 13 was rearranged, yielding

$$\frac{E - 3\upsilon_c RT}{T_e} = -h\frac{3\mu_c RT}{T_e} + E^0$$

From the slope of Figure 11, the junction fluctuation parameter $h = 1.2$ and from the intercept the equilibrium modulus for an infinite molecular weight, linear

polymer of similar chemical composition equaled $E° = 5.78 \times 10^8$ Pa. Moduli for the thermosetting specimens ranged from $0.5 \times 10^8$ to $3.5 \times 10^8$ Pa. For an affine network $h = 0$, and for a phantom network $h = 1$. The theory assumes long chains, segmental mobility, and permanence of structure.[13] Our structural epoxy does not necessarily satisfy these constraints, as evident by $h > 1$ and an intercept that seems a little large, but of the right order of magnitude. The high extent of cross-linking violates the requirement of long strands. Very few strand conformations are likely. The resin is highly aromatic and cyclic due to the epoxy and anhydride monomers. Thus, chain mobility is suspect. Chain mobility was enhanced by observing moduli at $T_g + 40$ °C. However, subject to a limited number of observations, data correlated, indicating that theoretical predictions of the rubber modulus seem to be in agreement with experimental data, even for dense, anhydride-cured epoxy networks. Research in progress is intensely exploring the effect of cross-linking with resins containing blends of PGE and DGEBA as well as initiator concentrations at high conversion levels.

## Summary

A chemical analysis of a structural epoxy resin was performed, yielding distributions of oligomeric and polymeric molecules within the sol. When compared with theoretical predictions based on a chain-growth polymerization, PDD's were in agreement in the lower to middle molecular weight fractions. Monomer decay dynamics were also observed to be consistent with theory for extensive conversions. Sol fractions were interpreted, yielding the extent of cross-linking. Data were then incorporated into cross-link node dynamics, yielding estimates of the number of elastically active junctions and strands at observed extents of cure. Predictions of the rubbery moduli were compared with experimental observations obtained through dynamic mechanical spectroscopy. Results are encouraging but suggest that additional research may be required to remove deficiencies noted.

Analyses concentrated on the effective concentration of unknown impurities and their effect on initiation/propagation kinetics. The impurity in DGEBA, believed to be 2,4-bis(α,α-dimethyl-*p*-hydroxylbenzyl)phenol, is expected to rapidly react with the anhydride and ultimately an oxirane. Thus, its immediate modeling effect is likely a modification to the initial condition used in Fukui and Yamabe's derivation.[6,7] In this regard, its difunctional nature would be expected to broaden, not narrow the population density distribution. It is dilute when compared to the concentrations of the added initiator and monomer DGEBA. Thus, its contribution has been lumped into hydroxyl type initiators including moisture in our discussion. However, if either of these materials was substantial, resulting reactions with the anhydride and subsequent propagation reactions are expected to yield a bimodal distribution, which was not observed. When the rate of initiation is distinct compared to the rate of propagation, Dotson et al.[1] and Chain and Timm[16] have shown with an analogous thermoplastic resin that the Gold[17] distribution converges to the Poisson[18] distribution with advancing conversion for this chain-growth cure. This is also expected for a mixture of similar initiators. Thus, the emphasis has been placed on the cumulative concentration of initiators lumped into a single rate expression. Analysis of monomer dynamics, gel points, and population density distributions emphasized their presence. This feedback demonstrates the utility of molecular analysis in the sense of quality control with thermosets.

For the molecular analysis of resins advanced past the point of gelation, specimens were subjected to leaching in an oven near their glass transition temperatures. Specimens were initially machined, forming flakes of less than 0.1 mm in thickness to create a high surface-to-volume ratio. The leaching step was conducted in stainless steel bombs for 2 h; however, heat transfer limitations result in solvent/solid temperatures approaching the oven temperature for only approximately 1 h. After exposure, up to 50% of the solvent is retained by the resulting, swollen gel. This solvent is distributed between the flakes and the flakes' interior. Research with relatively well cured composites and neat resin castings, such as those used in Figure 11, has shown that the materials extracted are very comparable to substances leached at ambient conditions for 2 months. The latter reached a state of equilibrium as confirmed by repeated GPC fractionations. Solvent penetration is relatively rapid and tends to quench reactions through specimen swelling. Diffusion is enhanced due to large scale, coordinated chain motions. Data are repeatable.

**Acknowledgment.** The authors acknowledge financial contributions from the Nebraska Research Initiative and the Center for Material Testing and Analysis.

## References and Notes

(1) Dotson, N. A.; Galvan, R.; Laurence, R. L.; Tirrell, M. *Polymer Process Modeling*; VCH Publishers: Cambridge, U.K., 1996.
(2) Graessley, W. W. *Polymeric Liquids & Networks: Structure and Properties*; Garland Science: Hamden, CT, 2003.
(3) Antoon, M. K.; Koenig, J. L. *J. Polym. Sci.* **1981**, *19*, 549.
(4) Nielsen, J. A.; Chen, S. J.; Timm, D. C. *Macromolecules* **1993**, *26*, 1369.
(5) Tadros, R.; Timm, D. C. *Macromolecules* **1995**, *28*, 7441.
(6) Robbins, D. J. Master's Thesis, University of Nebraska—Lincoln, 1996.
(7) Fukui, K.; Yamabe, T. *J. Polym. Sci.* **1964**, *A2*, 3743.
(8) Robbins, D. J.; Zhu, Q.; Timm, D. C. *Ind. Eng. Chem. Res.* **1997**, *36*, 1360.
(9) Gordon, M.; Ward, T. C.; Whitney, R. S. *Polymer Networks*; Chompf, A. J., Newman, S., Eds.; Plenum Press: New York, 1971.
(10) Gordon, M. *Proc. R. Soc. London* **1962**, *A268*, 240.
(11) Miller, D. R. *J. Polym. Sci., Part B: Polym. Phys.* **1988**, *26*, 1.
(12) Miller, D. R.; Macosko, C. W. *Macromolecules* **1978**, *11*, 656.
(13) Flory, P. J. *Principles of Polymer Chemistry*, Cornell University Press: Ithaca, NY, 1953.
(14) Flory, P. J. *Br. Polym. J.* **1985**, *17*, 96.
(15) Duering, E. R.; Kremer, K.; Grest, G. S. *Macromolecules* **1993**, *26*, 3241.
(16) Chian, W.; Timm, D. C. *Macromolecules* **2004**, *21*, 8091.
(17) Gold, L. *J. Chem. Phys.* **1958**, *28*, 91.
(18) Flory, P. J. *J. Am. Chem. Soc.* **1940**, *62*, 1561.
(19) Chian, W. Ph.D. Dissertation, University of Nebraska—Lincoln, 2002.
(20) Mark, E. J.; Erman, B. *Rubberlike Elasticity: A Molecular Primer*; J. Wiley & Sons: New York, 1988.
(21) Matějka, L.; Lovy, J.; Pokorný, S.; Bonchal, K.; Dušek, K. *J. Polym. Sci., Polym. Chem. Ed.* **1983**, *21*, 2873.
(22) Shiono, S.; Karino, I.; Ishimura, A.; Enomoto, J. *J. Chromatogr.* **1980**, *193*, 243.

(23) Dark, W. A.; Conrad, E. C.; Crossman, L. W., Jr. *J. Chromatogr.* **1974**, *91*, 247.
(24) Rozenberg, B. A. Epoxy Resins and Composites. In *Advances in Polymer Science*; Dušek, K., Ed.; Springer-Verlag: Berlin, 1986; Vol. 78, p 113.
(25) Luňák, S.; Vladyka, K.; Dušek, K. *Polymer* **1978**, *19*, 931.
(26) Cole, K. C. *Macromolecules* **1991**, *24*, 3093.
(27) Dušek, K. *Adv. Polym. Sci.* **1986**, *78*, 1.
(28) Mikeš, J.; Dušek, K. *Macromolecules* **1982**, *15*, 93.
(29) Charlesworth, J. M. *J. Polym. Sci., Polym. Phys. Ed.* **1979**, *17*, 1557, 1571.
(30) Charlesworth, J. M. *J. Polym. Sci., Polym. Phys. Ed.* **1980**, *18*, 621.

MA0492925